Mechanochemical Reactivity of Square Planar Nickel Complexes and Pyridyl Based Spacers for the Solid State Preparation of Coordination Polymers: The case of Nickel Diethyldithiophosphate and 4,4'-Bipyridine

Valentina Cabras,[a] Martina Pilloni, [a] Alessandra Scano, [a] Romina Lai, [a] Maria Carla Aragoni, [a] Simon J. Coles, [b] Guido Ennas* [a]

Abstract: The mechanochemical synthesis of a coordination polymer by using a preformed metal coordination complex and a pyridyl based spacer has been successfully performed. The (**1**·**L**)$_\infty$ coordination polymer has been rapidly obtained reacting the neutral square planar complex [((EtO)$_2$PS$_2$)$_2$Ni] (**1**) and 4,4'-bipyridine (**L**) at room temperature using two different mechanochemical approaches (Neat Grinding and Liquid Assisted Grinding method). The products were characterized by X-ray Powder Diffraction, IR Spectroscopy, Scanning Electron Microscopy, Thermogravimetry and Differential Scanning Calorimetry techniques. In parallel (**1**·**L**)$_\infty$ was prepared by conventional solvent-based methods and the X-Ray crystal structure of the polymer, obtained as a single crystal, compared to the mechanochemical data.

Introduction

Coordination polymers can be prepared by the self-assembly of naked metal ions or neutral metal complexes and donor molecules via coordination bonds and/or weaker interactions such as Van der Waals forces and H-bonds, and combine an intrinsic beauty to promising applications in fields as varied as gas storage, ion exchange, chemical sensing, catalysis, energy transfer, and separation.[1] The resulting assemblies can be directed by using as spacers between the metal nodes, organic molecules designed in order to have a pre-defined number of donor atoms in chosen positions, even if the flexibility of the ligand and different accessible conformations need to be examined and taken into account during design.[2] Moreover, in order to increase the overall control on the final structure, *cis*-protected metal building blocks or neutral coordinatively unsatured metal complexes can be used in place of naked ions, thus reducing the degrees of freedom of the system and avoiding the presence of counterions.[3]

A typical example of this building strategy has been reported successfully by Aragoni et.al.[4] by using neutral coordinatively unsaturated phosphonodithioato Ni(II) complexes, as neutral building blocks and bipyridyl-type as neutral ligands in a solution-based batch process. However, the properties of these crystalline materials are critically dependent on the deliberate creation of a crystalline network structure, planned using properly designed building blocks and this continues to be a challenge. The aspects to be evaluated in developing a network based on coordination polymers are the building blocks, i.e. metal nodes and organic spacers, the metal coordination environments, and also the formation conditions such as solvent, temperature, metal-ligand molar ratio, and weak secondary interactions.

In the last decades, mechanochemical methods based on grinding or ball-milling of the reactants have also been exploited in the field of crystal engineering.[5] These approaches have the aim of breaking and forming supramolecular interactions with no need for the intermediacy of a solvent, thus providing an alternative and green way to crystal engineering.

Mechanosynthesis, briefly defined by IUPAC as *a chemical reaction that is induced by the direct absorption of mechanical energy*,[6] is emerging as a powerful synthetic technique for environmentally-friendly and energy-efficient synthesis. It offers short reaction times, low-cost starting materials and avoids large quantities of solvent and high temperatures compared to conventional solvent-based methods.[7] Mechanosynthesis typically rapidly promotes solid state reactions and sometimes can induce improved reactivity of reagents resulting in new and unexpected reaction products. Furthermore, there are encouraging recent demonstration of industrial scale up.[8]

While mechanochemistry goes back nearly two centuries,[9] it is only in the last 30 years that the method has been developing in different broad areas of chemistry ranging from inorganic chemistry,[10] to organic,[11] supramolecular chemistry[9b] including the synthesis of coordination polymers,[12] and pharmaceutical solids.[13]

Mechanosynthesis can be carried out using manual (mortar and pestle) or non-manual methods such as extrusion or ball milling, the latter being the most widely used in the research laboratory.

Two different ball milling synthetic methods, called Neat Grinding (NG) and Liquid-Assisted Grinding (LAG or ILAG for ion LAG),[14] are known.[15] NG is a solvent-free method while in the LAG method small amounts of solvent are added to the solid reaction mixture. The reaction kinetics is often favoured by the presence of a liquid phase[15a, 16] and different structures can be obtained from the same precursors by changing solvents.[17] A careful solvent selection, as well as its accurate dosing, is therefore required.[18]

Mechanochemical methods normally provide microcrystalline powders and therefore single crystal diffraction methods can not usually be applied for structural characterization. X-ray powder diffraction is the main technique used to characterize microcrystalline powders although it remains more challenging than single crystal structure analysis in terms of deriving accurate structural information.[9b]

The problem can often be solved by growing single crystals by conventional solution-based methods and then comparing the resulting structure, via simulation of powder XRD patterns, with that formed by solid–solid mechanosynthesis.[19] It is worth noting that crystallization from solution and mechanical methods do not always yields the same product, especially when solvate species are formed and when nucleation of crystals is under solubility control.[20]

Several papers dealing with the synthesis of Coordination Polymers (CPs) and Metal Organic Frameworks (MOFs) by mechanochemical methods are reported in the literature. Many of these regards the synthesis of CPs/MOFs by ligand addition/exchange, ligand addition with elimination of a by-product or acid-base reaction of transition metal salts with appropriate ligands expanding the coordination sphere of the metal.[9b, 21] In other papers mechanochemical methods were adopted to induce a selective cleavage of bonds in coordination complexes compound giving rise to coordination unsatured compounds which can be used for a facile preparation of new coordination compounds in solution reaction and NG or LAG.[22]

Under these considerations and with the aim of finding new systems that could yield more predictable results, a systematic study to explore the mechanochemical reactions between neutral pre-formed coordination compounds and organic spacers was undertaken. Despite the mechanosynthesis of CPs has already been extensively investigated, to the best of our knowledge the mechanochemical synthesis by using neutral coordinatively unsatured dithiophosphato Ni(II) complexes has never been investigated before and could extend the rich of this field.

We present here a mechanochemical approach for reactions between neutral coordinatively unsatured O,O'-diethyl dithiophosphato Ni(II) complexes $[((EtO)_2PS_2)_2Ni]$ (**1**) and 4,4'-bipyridine (**L**), to yield a coordination polymer $(\mathbf{1}\cdot\mathbf{L})_\infty$. Moreover, conventional solvent-based synthesis of $(\mathbf{1}\cdot\mathbf{L})_\infty$ was also carried out in order to confirm its structure by single crystal analysis and compare it to that obtained by mechanosynthesis.

Results and Discussion

The reaction of 4,4'-bipyridine (**L**) and the nickel dithiophosphato complex $[Ni((EtO)_2PS_2)_2]$ (**1**) (Scheme 1) under solvothermal conditions afforded a crystalline compound which was isolated and identified by means of single crystal X-ray diffraction as the coordination polymer of formula $(\mathbf{1}\cdot\mathbf{L})_\infty$.

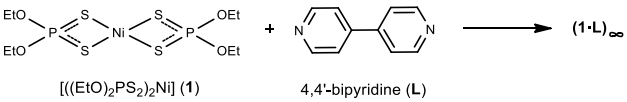

$[((EtO)_2PS_2)_2Ni]$ (**1**) 4,4'-bipyridine (**L**)

Scheme 1. General scheme of the reaction between complex **1** and ligand **L** to give $(\mathbf{1}\cdot\mathbf{L})_\infty$ coordination polymer.

Crystallographic data are reported in Table 1 and the asymmetric unit with selected bond lengths and angles in Fig. 1. Examination of the data reported in Table 1 shows a good agreement between the single crystal and powder data with minor discrepancies especially evident in the higher values of the c lattice parameter in the powder data. These differences can be ascribed to the free rotation of the ethoxy P-substituents that is evident even at 120 K (see thermal ellipsoid displacements of atoms C6-C9 in Fig.1) and become more evident at the temperature at which XRPD patterns were

[a] Dipartimento di Scienze Chimiche e Geologiche and INSTM units, Università di Cagliari, Cittadella Universitaria di Monserrato,09042 Monserrato (Cagliari), Italia
E-mail: ennas@unica.it
URL http://people.unica.it/guidoennas/

[b] Institution UK National Crystallography Service, Chemistry, University of Southampton, Highfield Campus, Southampton, United Kingdom

Supporting information for this article is given via a link at the end of the document.

recorded (298 K) giving rise to increasing disorder and therefore a minor packing efficiency.

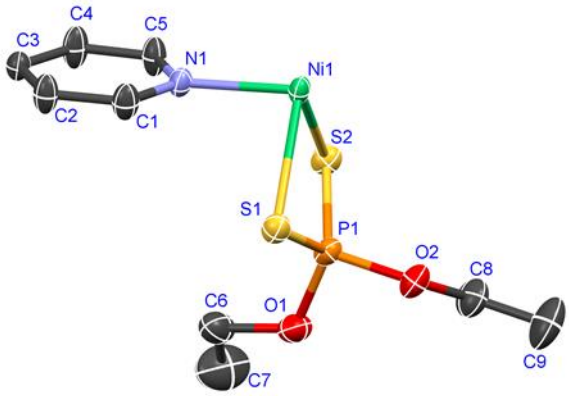

Figure 1. Ellipsoid drawing (70% probability level) of the asymmetric unit of (**1**·**L**)$_\infty$, with atom numbering scheme. Selected bond lengths and angles: Ni1–S1, 2.5057(8); Ni1–S2, 2.4948(7); Ni1–N1, 2.0750(17); P1–S1, 1.9769(8); P1–S2, 1.9821(8) Å; S1–Ni1–S2, 82.01(3); S1–Ni1–N1, 88.76(5); S2–Ni1–N1, 90.21(5)°.

Compound (**1**·**L**)$_\infty$ is a 1D polymer formed by axial coordination of **L** to the Ni^{II} ion of the square-planar dithiophosphato complex **1**. The [Ni(EtOPS$_2$)$_2$] units are bridged by the organic spacers **L** to form neutral parallel chains –**L**–[Ni(EtOPS$_2$)$_2$]–**L**–[Ni(EtOPS$_2$)$_2$]–**L**– as shown in Fig. 2. The coordination environment around the nickel ion results in a distorted octahedron with four sulfur atoms from two bidentate dithiophosphato units in the equatorial plane and two nitrogen atoms, from different bipyridine units, occupying the axial positions. The coordination of the neutral donor **L** induces variations in the bond distances and angles in the NiS$_4$ coordination framework similar to those found for analogous molecular adducts between phosphonodithioato complexes and pyridine derivatives, which is ascribed to the reduced net positive charge on the central Ni[4b]. As shown in Fig. 2a, the main structural feature of (**1**·**L**)$_\infty$ is the presence of linear chains that closely resemble the analogous polymer [Ni(EtOdtp)$_2$**L**]$_\infty$ formed by reacting the dithiophosphonato complex [Ni(EtOdtp)$_2$] [where EtOdtp = (4-MeOPh)(EtO)PS$_2$] with **L**.[4a] The Ni···Ni distances between bridged dithiophosphato units of 11.24 Å are very similar to those of 11.38 Å found in [Ni(EtOdtp)$_2$**L**]$_\infty$. The chains are aligned in planes that pack in an antiparallel fashion (shown in blue and yellow in Fig. 2b) due to the presence of glide planes perpendicular to the (010) direction with glide component (1/2, 0, 1/2).

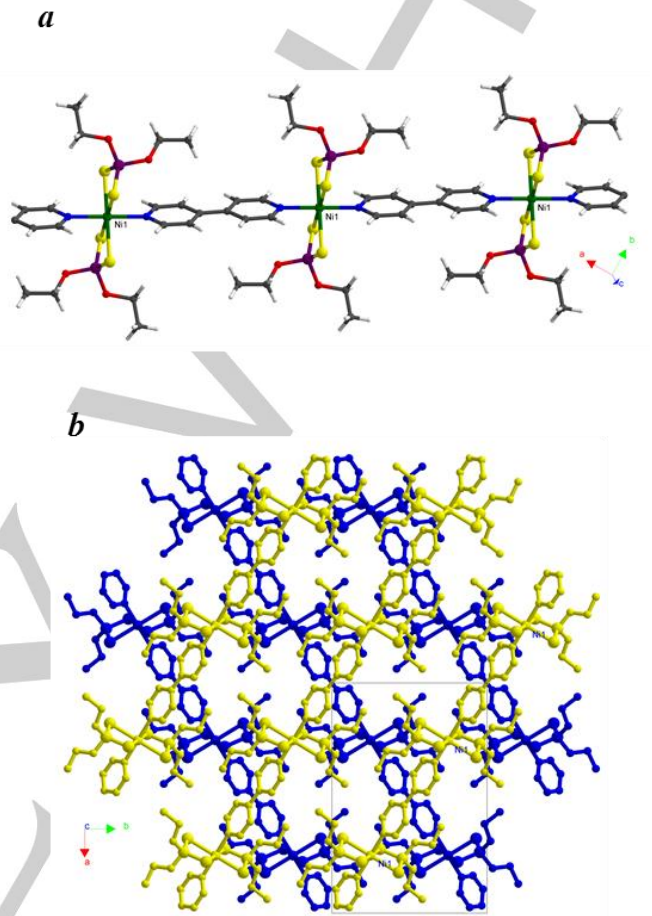

Figure 2: Packing views of (**1**·**L**)$_\infty$ showing the linear polymeric chain (***a***) and the parallel planes packing in the different directions (evidenced in blue and yellow color) due to the presence of glide planes perpendicular to the (010) direction with glide component (1/2, 0, 1/2) (***b***).

Coordination polymer (**1**·**L**)$_\infty$ could also be prepared mechanochemically by grinding the powders of **1** with **L** in the ball milling apparatus.[23] The complexity of the milling process can be simplified in two different elemental mechanical actions by which energy is transferred from the milling tools to the milled powder: collision and attrition. The mechanism of collision prevails when the milling device contains a limited number of balls. On the contrary it is expected that the attrition mechanism prevails when the mill begins to be filled up with balls.[24] In all our experiments the collision regime is dominant respect to the attrition one.[25] However, although several studies are already published, the mechanism of the mechanochemical processes, which gives rise to the products, remains an open research field. [15b, 16b, 26]

Table 1. Summary of X-Ray single crystal and powder data and structure refinements parameters for compound (**1**·**L**)$_\infty$ obtained by conventional and grinding methods (NG 10 min and LAG 5 min). (<D> average crystal size; σ microstrain)

Compound	(**1**·**L**)$_\infty$ conv solv-based sample	(**1**·**L**)$_\infty$ conv solv-based sample	(**1**·**L**)$_\infty$ NG 10 min	(**1**·**L**)$_\infty$ LAG 5 min
XRD method	single crystal	powder	powder	powder
Crystal system	monoclinic	monoclinic	monoclinic	monoclinic
Space group	C 2/c	C 2/c	C 2/c	C 2/c
a / Å	19.099(4)	19.71(2)	19.78(2)	19.74(2)
b / Å	11.842(2)	11.25(2)	11.24(2)	11.23(2)
c / Å	12.957(3)	14.15(2)	14.36(2)	14.24(2)
β / °	112.93(3)	116.7(5)	116.8(5)	116.7(5)
V / Å^3	2698.9(11)	2776(3)	2848(3)	2820(3)
Z	4	4	4	4
T / K	120	298	298	298
D_{calc} /g cm^{-3}	1.441	-	-	-
θ min-max /°	3.3-27.5	5-80	5-80	5-80
<D> / nm	-	>100	37	60
σ / %	-	<0.1	0.6	0.4
Wavelength/ Å	0.71073 (MoKα)	1.54056 (CuK α)	1.54056 (CuK α)	1.54056 (CuK α)
R indices (all data)	R_1 = 0.030; wR_2 = 0.0705	R_{wp}=10.0	R_{wp}=9.2	R_{wp}=5.8

$$w^{-1} = \left[\sigma^2\left(F_{exp}^2\right) + (0.0320P)^2 + 2.1046P\right] \ where\ P = [F_{exp}^2 + 2F_{calc}^2];$$

$$R_1 = \sum_{i=1}^{n}(|F_{exp,i}| - |F_{calc,i}|)/\sum_{n=1}^{\infty}|F_{exp,i}|;$$

$$wR_2 = \left\{\sum_{i=1}^{n}[w(F_{exp,i}^2 - F_{calc,i}^2)^2]/\sum_{n=1}^{\infty}[w(F_{exp,i}^2)^2]\right\}^{1/2};$$

$$R_{wp} = 100 * \sum_{i=1}^{n} w_i \left(I_i^{exp} - I_i^{calc}\right)^2 / \sum_{i=1}^{n}\left(w_i I_i^{exp}\right)^2.$$

The XRPD patterns recorded on samples at different selected time intervals during the mechanosynthesis are shown in Figure S1. After 5 min of milling the pattern (showed in Fig. S1 a) indicates the almost complete formation of coordination polymer (**1**·**L**)$_\infty$. However, small peaks due to reagents were barely evident, particularly faint peaks at 8.78, 12.19 and 13.51 2θ degrees due to nickel complex **1** and peaks at 12.57 and 25.62 2θ degree belonging to **L**. After 10 min milling the complete conversion of reagents into the green colored (**1**·**L**)$_\infty$ compound was achieved. Its pattern corresponds to that recorded for the coordination polymer obtained by conventional solvent-based methods (Fig. 3 c and a, respectively), with no residual peaks due to unreacted reagents detectable.

Rietveld refinement (Fig. S3) of the NG XRPD pattern indicated a good agreement with the experimental structure obtained from powder structure solution of the sample prepared in the conventional solvent-based manner (Table 1). The isotropic size-strain model indicated an average crystal size of 37 nm and a 0.6% microstrain for the NG sample which contributed to slight packing difference compared to conventional solvent-based sample.

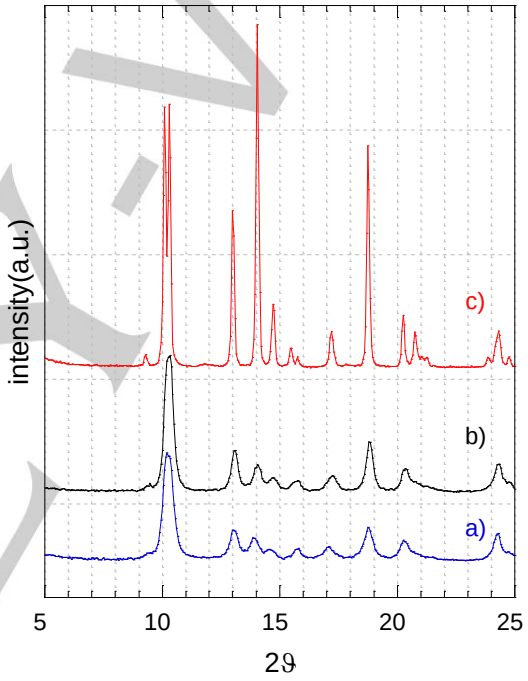

Figure 3: Comparison of XRD patterns for compound (**1**·**L**)$_\infty$ obtained by a) NG after 10 minutes grinding, b) LAG after 5 minutes grinding and c) conventional solvent-based synthesis samples.

Further milling of the powder did not change the structure of the products and therefore at 10 min of milling the synthesis can be considered as having concluded (Fig. S1 a-e). It is noteworthy that the XRPD peaks for the NG 10 minute sample are in the same position as the conventionally prepared sample, but the intensity and width, and therefore size and strain, are significantly different. This can be explained by the continuous reduction of crystallite grain size, due to the repeated fracture of the powders induced by milling, accompanied by progressive dispersion and intimate mixing at the atomic level, which promotes interdiffusion of the starting compounds and their solid

state reaction. Moreover milling induces structural disorder giving broader peaks with different intensities.

With the aim of optimizing the synthesis, we also explored the LAG method by adding a few microlitres of ethanol, normally used as solvent in the conventional solvent-based synthesis, to the starting powder reagents. Examination of Figure 3b shows that the use of solvent reduced the reaction times: LAG mechanosynthesis can be considered concluded after 5 minutes of milling (Fig. S2 a-d). The 5 minute LAG XRPD pattern is very similar to the 10 minute NG synthesis (Fig. 3a-b). Rietveld refinement (Fig. S3 and Table 1) of the LAG sample indicated an average crystal size of 60 nm, which is slightly bigger than the NG sample. The microstrain of the LAG sample is very similar to the corresponding NG sample.

The FTIR spectra of the samples obtained by NG, LAG and conventional solvent-based methods are reported in Fig. S4. The most characteristic ring vibration v(C-N), v(C-C) and pirydine breathing mode can be observed in the range (cm^{-1}): 1600.0-1608.9, 1533.4-1537.5 and 1006.8-1018.3, respectively. These bands are shifted at higher frequencies compared to free 4,4'-bipy[27], thus confirming 4,4'-bipy coordination to the nickel metal complex.

SEM micrographs of the compound (**1**·**L**)$_\infty$ prepared by conventional solvent-based synthesis and using NG and LAG mechanosyntesis methods highlight the different morphology of the samples (Fig. 4): the conventional solvent-based sample is mainly constituted of well-defined microcrystals (left), whilst NG and LAG samples show irregular shaped aggregates of nanocrystals with rough surfaces. Moreover the LAG sample forms as smaller aggregates in comparison to the NG sample.

In order to determine the thermal behavior of the samples TGA and DSC measurements were conducted on compound (**1**·**L**)$_\infty$ prepared by conventional solvent-based, and mechanochemical NG and LAG methods (Fig. 5).

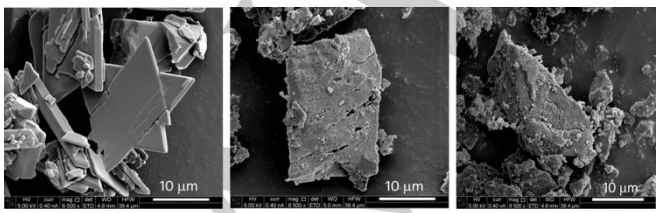

Figure 4: SEM images of compound (**1**·**L**)$_\infty$: micro-crystals from conventional solvent-based synthesis (left), NG sample after 10 minutes grinding (middle), LAG sample after 5 minutes grinding (right). Magnifications are reported in the bottom of the micrograph (bar= 10µm).

TG and the corresponding derivative dTG curve of the sample prepared by conventional solvent-based synthesis (Figure 4a left) shows three main mass loss (and dTG peaks) in the temperature range of i) in the range 217-241, (ii) 339-466 °C and (iii) 780-957°C. The first and second steps of the TG curve reflect thermal decomposition of the organic parts of (**1**·**L**)$_\infty$; the mass remaining after the first step (73.9%) corresponds, as expected, to the loss of **L**. The plateau observed from 466 to 780 °C is consistent with the presence of the bis(dithio-metaphosphato) nickel(II) [$Ni(S_2PO)_2$] moiety, in agreement with the data reported in literature for the analogous [$Pt(EtOPS_2)_2$] platinum complex. [28]

At higher temperature, decomposition of the sample is observed, with formation of a residue product identified as nickel phosphate $Ni_2P_2O_7$ by XRPD analysis (data not shown).

In Fig. 5 (right side) DSC thermograms of (**1**·**L**)$_\infty$ samples are also reported, along with those of **L** and **1** reagents for comparison. In agreement with the TG analysis, the DSC curve of the conventional solvent-based sample shows a no reversible asymmetric exothermic peak at 223°C due to decomposition of (**1**·**L**)$_\infty$ into [$Ni(S_2PO)_2$]. No peaks are observed in the DSC curve at temperatures lower than 220°C indicating that the polymer (**1**·**L**)$_\infty$ is stable up to this temperature.

Similar thermal behaviors were observed for the samples obtained by mechanochemical NG (b) and LAG (c) methods (Fig. 5, left), with formation of the same degradation compounds, with small differences only in the temperature of the first step, which is slightly lower (196 °C) in comparison to that found for the conventionally prepared sample (220 °C). The corresponding DSC exothermic peaks are in agreement, with a shift of temperature from 223 to 209 °C. Moreover, in ball milled samples, particularly the NG one, the DSC peaks due to polymer decomposition are broader than those recorded for the conventional solvent-based sample, which is consistent with smaller and/or more disordered (**1**·**L**)$_\infty$ particles.

Synthesis with a 2:1 - **L**:**1** molar ratio was also carried out in order to evaluate the existence of compounds with different stoichiometry, but even after a long milling time (20 minutes) coordination polymer (**1**·**L**)$_\infty$ was the only compound obtained. The XRPD pattern of this sample (Fig. S5) shows peaks due to excess **L**, thus confirming the presence of unreacted reagent. DSC measurement (Fig. S6) confirmed the presence of unreacted **L**, showing an endothermic peak assignable to **L** melting. Moreover, after washing with ethanol and drying, the

milled powder was analyzed by XRPD and DSC (S5 and S6) confirming its (**1**·**L**)$_\infty$ nature.

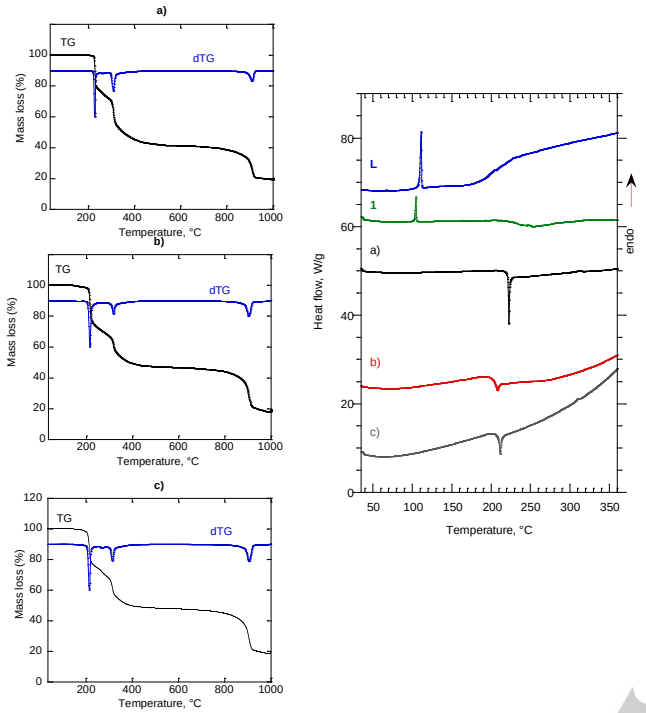

Figure 5: TG and dTG curves (left side) and DSC (right side) of compound (**1**·**L**)$_\infty$ obtained with a) conventional, b) NG and c) LAG methods. In DSC plots, **L** and **1** thermograms were also reported for comparison.

Conclusions

Mechanochemical reaction of neutral O,O'-diethyldithiophosphato Ni^{II} complex (**1**) with 4,4'-bipyridine (**L**) allows the formation of a 1D coordination polymer (**1**·**L**)$_\infty$. This coordination polymer can also be obtained by conventional, solution-based, synthesis. The mechanochemical protocol developed gave (**1**·**L**)$_\infty$ polymer with significant benefits compared to solution-based protocols and confirmed the 'green' nature of this methodology: reactions are much faster (less than one hour compared to several hours) and the use of high temperatures and solvents are avoided. The NG mechanochemical approach gives yields comparable to those obtained from LAG but the latter is more efficient at reducing the reaction time. Moreover, as well known in the literature, [29] the solvent acts as a 'lubricant' for kinetic acceleration of the reaction, as a heat sink for exothermic reactions, as a dispersant for product removal from the reaction sites, as a suspending agent for the reactants, and as a crystallization promoter. As a consequence, the average crystal size in the LAG sample is slightly larger than that obtained in NG samples.

Further systematic work is now in progress in our laboratory with the aim of studying mechanochemical synthesis of coordination polymers starting from different metal complexes with different bipyridyl-based spacers.

Experimental Section

4,4'-bipyridine ($C_{10}H_8N_2$, 99%, Sigma-Aldrich) was used as received without further purification. The dithiophosphato complex [$((EtO)_2PS_2)_2Ni$] (**1**) was synthesized according to the literature procedure.[30] The mixture of reagents was milled using a shaker ball-mill (Spex 8000, CertiPrep, Metuchen, NJ) in a 30 mL teflon coated stainless-steel grinding jar. Two 5 mm diameter zirconia balls (0.40 g) were used. In order to prevent excessive overheating of the jar the experiments were carried out alternating milling and rest period at 5 min intervals. In the LAG synthesis ethanol (96%, Sigma-Aldrich, without further purification) was used as the solvent. The effect of milling was monitored by X-ray powder diffraction (XRPD) performed on small portions of the powder sampled at different milling times. XRPD patterns were recorded at 40 kV and 30 mA on a Seifert X3000 diffractometer using CuK_α radiation in Bragg Brentano geometry and equipped with a graphite monochromator and scintillation counter. The data were collected between 5.00 and 80.00° 2θ, with a 0.05° 2θ step size. In order to obtain a satisfactory signal-to-noise ratio in the X-ray pattern an appropriate acquisition time was selected. The CSD [31] was used to compare experimental and deposited structures. The Maud software [32] was used for Rietveld refinements, and the peak profiles were modelled by using the pseudo-Voigt profile function. Recommended fitting procedures were adopted and the instrumental profile broadening was derived from the fitting of XRPD data obtained from standard samples.[33] The scale factor, background contribution, lattice parameter, unit cell, average crystallite size, micro-strain were refined. The R_{wp}-factor was used as an indicator of goodness of fit.

X-ray structure determinations and crystallographic data for compound (**1**·**L**)$_\infty$ were collected at 120(2) K by means of combined phi and omega scans on a Bruker-Nonius Kappa CCD area detector, situated at the window of a FR591rotating anode (graphite Mo-K_α radiation, λ = 0.71073Å). The structures were solved by direct methods, SHELXS-97 and refined on F^2 using SHELXL.[34]

Anisotropic displacement parameters were assigned to all non-hydrogen atoms. Hydrogen atoms were included in the refinement, but thermal parameters and geometry were constrained to ride on the atom to which they are bonded. The data were corrected for absorption effects using SORTAV.[35]

The structure has been deposited with the Cambridge Crystallographic Data Centre: deposition number CCDC 1517440.

Sample morphology was observed using scanning electron microscopy (SEM) (S-4100, HITACHI). The samples were fixed on a brass stub using

carbon double-sided, coated with gold blazers SCD 004 sputter coater for 2 min and observed under an excitation voltage of 10 kV.

FT-Infrared spectra were recorded on a Thermo Nicolet 5700 spectrometer at room temperature using a flow of dried air. Middle IR spectra (resolution 4 cm^{-1}) were recorded as KBr pellets, with a KBr beam-splitter and KBr windows.

FT-Raman spectra (resolution of 4 cm^{-1}) were recorded as KBr solid mixture on a Bruker RFS100 FT-Raman spectrometer, fitted with an In-Ga-As detector (room temperature) operating with a Nd-YAG laser (excitation wavelength 1064 nm) with a 180° scattering geometry. The excitation power was modulated between 100 and 250 mW.

Elemental analyses were performed with an EA1108 CHNS-O Fisons instrument.

Differential scanning calorimetry (DSC) measurements were performed at atmospheric pressure using a Perkin-Elmer instrument model DSC7 having a maximum temperature detectable of 600°C using crimped aluminum crucible. The measurements were performed under Ar flow (40 mL min^{-1}). Samples of 5 mg were encapsulated in aluminum crucibles and scanned with a heating rate of 10°C min^{-1} in the temperature range of 40–360 °C where the most significant transformation are present. The calorimeter was calibrated by measuring the melting temperature of metallic indium and zinc (99.999 mass% purity) and the temperature was obtained with an accuracy of ±0.5 °C.

Thermogravimetric analysis was carried out on a TGA-SDTA 851 Mettler-Toledo instrument using an alumina sample pan under Argon flow (50 mL min^{-1}) with a heating rate of 10 K min^{-1} in the temperature range 40-1000°C. The instrument was calibrated with zinc and iron standard samples and the temperature was obtained with an accuracy of ±2 °C.

Syntheses of $[((EtO)_2PS_2)_2Ni{\cdot}L)]_\infty$, $(1{\cdot}L)_\infty$.

Conventional solvent-based synthesis: complex **1** (21.4 mg, 0.05 mmol) and **L** (7.8 mg, 0.05 mmol) were reacted at 140 °C in a high pressure Aldrich tube in 30 mL of EtOH. After complete dissolving of the reagents, the reaction mixture was slowly cooled to room temperature. After a few days $(\mathbf{1{\cdot}L})_\infty$ (13.0 mg, 0.02 mmol, 47% yield) was obtained as green crystals suitable for X-ray analysis. M.p.: 210 °C (d). Elemental analysis found (calc. for $C_{18}H_{26}N_2O_4P_2S_4Ni$; formula mass = 585.31 Da): C, 36.98 (36.94); H, 4.40 (4.82); N, 4.83 (4.79); S, 19.71 (21.91). FT-IR (KBr, 4000-400 cm^{-1}): 2974 vw, 2284 vw, 1608 s, 1535 vw, 1490 w, 1409 m, 1388 w, 1221 m, 1160 w, 1070 vw, 1042 s, 1018 vs, 956 vs, 815 vs, 774 s, 729 w, 682 s, 665 m, 634 vm, 552 w, 482 vm, 470 m, 452 w, 440 w 426 m, 412 w cm^{-1}. FT-Raman (3500-100 cm^{-1}, 200 mW, solid in KBr, relative intensities between parentheses related to the highest peak taken equal to 10.0): 2928 (3.5), 1614 (10), 1295 (9.8), 1022 (7.2), 550 (3.5), 92 (6.3) cm^{-1}.

NG synthesis: equimolar quantities of complex **1** (0.1712g, 0.4 mmol) and **L** (0.0637g, 0.4mmol) were placed in the jar. The NG synthesis was also performed in the 2:1 (**L**:**1**) molar ratio, and the resulting product compared to those obtained by conventional and equimolar NG synthesis.

LAG synthesis: equimolar quantities of complex **1** (0.1712g, 0.4 mmol) and **L** (0.0637g, 0.4mmol) were placed in the jar along with 50 µL of ethanol.

Acknowledgements

Authors wish to thank the Dipartimento di Scienze Chimiche e Geologiche of the Università degli Studi di Cagliari and Fondazione di Sardegna for financial support (PRID 2015 and FdS/RAS 2016). V.C. kindly acknowledge Sardinia Regional Government (P.O.R. Sardegna, European Social Fund 2007-2013/Axis IV Human Resources objective 1.3, line of activity 1.3.1.) for PhD financial program. G.E. wish to thank CRS4 for assistance in SEM measurements.

Keywords: Mechanochemistry• Solid State Reaction • Coordination Polymers • Crystal Engineering • Green Chemistry

[1] a) J. Fernández-Catalá, M. E. Casco, M. Martínez-Escandell, F. Rodríguez-Reinoso, J. Silvestre-Albero, *Microporous Mesoporous Mater.***2017**, *237*, 74-81; b) Y. Gao, S. Li, Y. Li, L. Yao, H. Zhang, *Appl. Catal. B: Environmental* **2017**, *202*, 165-174; c) N. Yin, K. Wang, L. Wang, Z. Li, *Chem. Eng. J.* **2016**, *306*, 619-628.

[2] a) D. K. Chand, M. Fujita, K. Biradha, S. Sakamoto, K. Yamaguchi, *Dalton Trans.* **2003**, 2750-2756; b) M. Fujita, *Chem. Soc. Rev.* **1998**, *27*, 417-425; c) S. Leininger, B. Olenyuk, P. J. Stang, *Chem. Rev.* **2000**, *100*, 853-908; d) B. Olenyuk, J. Whiteford, *J. Chem. Soc., Dalton Trans* **1998**, *1707*; e) L. R. MacGillivray, *Metal-organic frameworks: design and application*, John Wiley & Sons, **2010**.

[3] a) C. B. Aakeröy, J. Desper, J. Valdés-Martínez, *CrystEngComm* **2004**, *6*, 413-418; b) M. C. Aragoni, M. Arca, F. A. Devillanova, M. B. Hursthouse, S. L. Huth, F. Isaia, V. Lippolis, A. Mancini, S. Soddu, G. Verani, *Dalton Trans.* **2007**, 2127-2134; c) K. Biradha, M. Sarkar, L. Rajput, *Chem. Commun.* **2006**, 4169-4179; d) D. Braga, L. Brammer, N. R. Champness, *CrystEngComm* **2005**, *7*, 1-19; e) L. Brammer, *Chem. Soc. Rev.* **2004**, *33*, 476-489; f) M. E. Braun, C. D. Steffek, J. Kim, P. G. Rasmussen, O. M. Yaghi, *Chem. Commun.* **2001**, 2532-2533; g) Z.-F. Chen, S.-F. Zhang, H.-S. Luo, B. F. Abrahams, H. Liang, *CrystEngComm* **2007**, *9*, 27-29; h) A.-L. Cheng, N. Liu, Y.-F. Yue, Y.-W. Jiang, E.-Q. Gao, C.-H. Yan, M.-Y. He, *Chem. Commun.* **2007**, 407-409; i) F. A. Cotton, C. Lin, C. A. Murillo, *Acc. Chem. Res.* **2001**, *34*, 759-771; j) E.-Q. Gao, S.-Q. Bai, Z.-M. Wang, C.-H. Yan, *Dalton Trans.* **2003**, 1759-1764; k) I.Goldberg, *Chem. Commun.* **2005**, 1243-1254; l) S. Kitagawa, R. Kitaura, S. i. Noro, *Angew. Chem. Int. Ed.* **2004**, *43*, 2334-2375; m) W. Lu, Z. Wei, Z.-Y. Gu, T.-F. Liu, J. Park, J. Park, J. Tian, M. Zhang, Q. Zhang, T. Gentle III, *Chem. Soc. Rev.* **2014**, *43*, 5561-5593; n) M. O'Keeffe, M. Eddaoudi, H. Li, T. Reineke, O. M. Yaghi, *J. Solid State Chem.* **2000**, *152*, 3-20; o) B. Rather, M. J. Zaworotko, *Chem. Commun.* **2003**, 830-831; pN. L. Rosi, M. Eddaoudi, J. Kim, M. O'Keeffe, O. M. Yaghi, *CrystEngComm* **2002**, *4*, 401-404; qS. Sain, T. K. Maji, G. Mostafa, T.-H. Lu, N. R. Chaudhuri, *New J. Chem.* **2003**, *27*, 185-187.

[4] a) M. C. Aragoni, M. Arca, N. R. Champness, A. V. Chernikov, F. A. Devillanova, F. Isaia, V. Lippolis, N. S. Oxtoby, G. Verani, S. Z. Vatsadze, *Eur. J. Inorg. Chem.* **2004**, *2004*, 2008-2012; b) M. C. Aragoni, M. Arca, N. R. Champness, M. De Pasquale, F. A. Devillanova, F. Isaia, V. Lippolis, N. S. Oxtoby, C. Wilson, *CrystEngComm* **2005**, *7*, 363-369.

[5] L. Aboutorabi, A. Morsali, *Coord. Chem. Rev.* **2016**, *310*, 116-130.

[6] A. D. McNaught, A. Wilkinson, **1997**.

[7] D. Prochowicz, K. Sokołowski, I. Justyniak, A. Kornowicz, D. Fairen-Jimenez, T. Friščić, J. Lewiński, *Chem. Commun.* **2015**, *51*, 4032-4035.

[8] F. Carli, *Proc. Int. Symp. Controlled Release Bioact. Mater.* **1999**, *26*, 873.

[9] a) G. A. Bowmaker, *Chem. Commun.* **2013**, *49*, 334-348; b) S. L. James, C. J. Adams, C. Bolm, D. Braga, P. Collier, T. Friščić, F. Grepioni, K. D. Harris, G. Hyett, W. Jones, *Chem. Soc. Rev.* **2012**, *41*, 413-447.

[10] M. Pilloni, J. Nicolas, V. Marsaud, K. Bouchemal, F. Frongia, A. Scano, G. Ennas, C. Dubernet, *Int. J. Pharm.* **2010**, *401*, 103-112.

[11] a) L. Chen, B. E. Lemma, J. S. Rich, J. Mack, *Green Chemistry* **2014**, *16*, 1101-1103; b) B. P. Biswal, S. Chandra, S. Kandambeth, B. Lukose, T. Heine, R. Banerjee, J*ournal of the American Chemical Society* **2013**, 135, 5328-5331; c) V. Stilinović, D. Cinčić, M. Zbačnik, B. Kaitner, *Croatica Chemica Acta* **2012**, 85, 485-493.

[12] a) D. Braga, S. L. Giaffreda, F. Grepioni, A. Pettersen, L. Maini, M. Curzi, M. Polito, *Dalton Trans.* **2006**, 1249-1263; b) M. Pilloni, F. Padella, G. Ennas, S. Lai, M. Bellusci, E. Rombi, F. Sini, M. Pentimalli, C. Delitala, A. Scano, *Microporous Mesoporous Mater.***2015**, *213*, 14-21.

[13] a) D. Braga, L. Maini, F. Grepioni, *Chem. Soc. Rev.* **2013**, *42*, 7638-7648; b) M. Pilloni, G. Ennas, M. Casu, A. M. Fadda, F. Frongia, F. Marongiu, R. Sanna, A. Scano, D. Valenti, C. Sinico, *Pharm. Develop. Tecnol.* **2013**, *18*, 626-633.

[14] T. Friščić, A. V. Trask, W. Jones, W. Motherwell, *Angew. Chem.* **2006**, *118*, 7708-7712.

[15] a)T. Friščić, L. Fábián, *CrystEngComm* **2009**, *11*, 743-745; b) A. Pichon, S. L. James, *CrystEngComm* **2008**, *10*, 1839-1847.

[16] a) T. Friščić, D. G. Reid, I. Halasz, R. S. Stein, R. E. Dinnebier, M. J. Duer, *Angew. Chem.* **2010**, *122*, 724-727; b) N. Shan, F. Toda, W. Jones, *Chem. Commun.* **2002**, 2372-2373.

[17] a) H. Yang, S. Orefuwa, A. Goudy, *Microporous Mesoporous Mater.* **2011**, *143*, 37-45; b) D. Cinčić, B. Kaitner, *CrystEngComm* **2011**, *13*, 4351-4357.

[18] W. Yuan, T. Friščić, D. Apperley, S. L. James, *Angew. Chem.* **2010**, *122*, 4008-4011.

[19] D. Braga, L. Maini, G. de Sanctis, K. Rubini, F. Grepioni, M. R. Chierotti, R. Gobetto, *Chem. Eur. J.* **2003**, *9*, 5538-5548.

[20] A. V. Trask, J. van de Streek, W. S. Motherwell, W. Jones, *Crystal growth & design* **2005**, *5*, 2233-2241.

[21] a) C. J. Adams, H. M. Colquhoun, P. C. Crawford, M. Lusi, A. G. Orpen, *Angew. Chem.* **2007**, *119*, 1142-1146; b) C. J. Adams, M. F. Haddow, M. Lusi, A. G. Orpen, *Proc. Nat. Acad. Sci.* **2010**, *107*, 16033-16038; c) M. Lusi, J. L. Atwood, L. R. MacGillivray, L. J. Barbour, *CrystEngComm* **2011**, *13*, 4311-4313; d). Prochowicz, I. Justyniak, A. Kornowicz, T. Kaczorowski, Z. Kaszkur, J. Lewiński, *Chemistry–A European Journal* **2012**, 18, 7367-7371.

[22] K. Užarević, M. Rubčić, M. Radić, A. Puškarić, M. Cindrić, *CrystEngComm* **2011**, *13*, 4314-4323.

[23] The SPEX 800 shaker mill is a vibratory mill, where its jar is moved at a high frequency cycle that involves motion in three orthogonal directions and where rotation and vibration have the same frequency.

[24] M. Magini, A. Iasonna, *Mater. Trans., JIM, JIM* **1995**, *36*, 123-133.

[25] T. P. Yadav, R. M. Yadav, D. P. Singh, *Nanosci. Nanotech.* **2012**, *2*, 22-48.

[26] a) E. Boldyreva, *Chemical Society Reviews* **2013**, 42, 7719-7738; b) O. Dolotko, J. W. Wiench, K. W. Dennis, V. K. Pecharsky, V. P. Balema, New Journal of Chemistry 2010, 34, 25-28.

[27] D. Czakis-Sulikowska, J. Kałużna, *J. Therm. Anal. Calorim.* **1996**, *47*, 1763-1776.

[28] T. A. Rodina, A. V. Ivanov, A. V. Gerasimenko, I. A. Lutsenko, M. A. Ivanov, J. V. Hanna, O. N. Antzutkin, V. I. Sergienko, *Polyhedron* **2011**, *30*, 2210-2217.

[29] T. Friščić, S. L. James, E. V. Boldyreva, C. Bolm, W. Jones, J. Mack, J. W. Steed, K. S. Suslick, *Chem. Commun.* **2015**, *51*, 6248-6256.

[30] a) V. G. Albano, M. C. Aragoni, M. Arca, C. Castellari, F. Demartin, F. A. Devillanova, F. Isaia, V. Lippolis, L. Loddo, G. Verani, *Chem. Commun.* **2002**, 1170-1171; b) M. C. Aragoni, M. Arca, F. A. Devillanova, J. R. Ferraro, F. Isaia, F. Lelj, V. Lippolis, G. Verani, *Can. J. Chem.* **2001**, *79*, 1483-1491; c) M. Caria Aragoni, M. Arca, F. Demartin, F. A. Devillanova, C. Graiff, F. Isaia, V. Lippolis, A. Tiripicchio, G. Verani, *Eur. J. Inorg. Chem.* **2000**, 2239-2244.

[31] C. R. Groom, I. J. Bruno, M. P. Lightfoot, S. C. Ward, *Acta Crystallogr., Sect. B: Struct. Sci* **2016**, *72*, 171-179.

[32] L. Lutterotti, S. Matthies, H. Wenk, *IUCr: Newsletter of the CPD* **1999**, *21*.

[33] R. Young, *The Rietveld Method* **1993**, *5*, 1-38.

[34] a) G. Sheldrick, *Acta Crystallogr., Sect. A: Found. Crystallogr.* **2008**, *64*, 112-122; b) G. M. Sheldrick, *Acta Crystallogr., Sect. C: Cryst. Struct. Commun.* **2015**, *71*, 3-8.

[35] a) R. H. Blessing, *Acta Crystallogr., Sect. A: Found. Crystallogr.* **1995**, *51*, 33-38; b) R. H. Blessing, *J. Appl. Crystallogr.***1997**, *30*, 421-426.

FULL PAPER

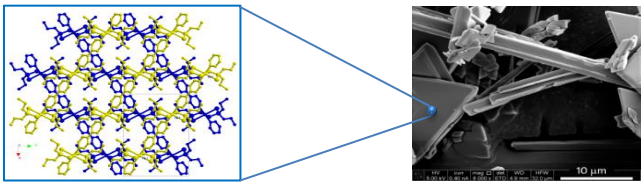

An environmental friendly one pot mechanosynthesis of a Ni(II) coordination polymer starting from a Square Planar Nickel Complexes and a pyridyl based spacer, the coordinatively unsatured dithiophosphato Ni(II) complex $[((EtO)_2PS_2)_2Ni]$ along with 4,4'-bipyiridine has been developed.

Ni(II)-Dithiophosphato Coordination Polymers

V. Cabras,[a] M. Pilloni,[a] A. Scano,[a] R. Lai,[a] M. C. Aragoni,[a] S. J. Coles,[b] G. Ennas[a]*

Page No. – Page No.

Mechanochemical Reactivity of Square Planar Nickel Complexes and Pyridyl Based Spacers for the Solid State Preparation of Coordination Polymers: The case of Nickel Diethyldithiophosphate and 4,4'-Bipyridine